Articles

Detection of an Equilibrium Intermediate in the Folding of a Monomeric Insulin Analog

Christopher Bryant,[‡,⊥] Margaret Strohl,[§] L. Kenney Green,[∥] Harlan B. Long,[∥] Leila A. Alter,[‡] Allen H. Pekar,[‡] Ronald E. Chance,[∥] and David N. Brems*[,‡]

Parenteral Products Research and Development, Physical Chemistry, and Diabetes Research, Eli Lilly & Company, Lilly Corporate Center, Indianapolis, Indiana 46285

Received August 2, 1991; Revised Manuscript Received March 19, 1992

ABSTRACT: To determine the conformational properties of the C-terminal region of the insulin B-chain relative to the helical core of the molecule, we have investigated the fluorescence properties of an insulin analog in which amino acids B28 and B29 have been substituted with a tryptophan and proline residue respectively, ([W_{B28},P_{B29}]insulin). The biological properties and far-UV circular dichroism (CD) spectrum of the molecule indicate that the conformation is similar to that of native human insulin. Guanidine hydrochloride (GdnHCl)-induced equilibrium denaturation of the analog as monitored by CD intensity at 224 nm indicates a single cooperative transition with a midpoint of 4.9 M GdnHCl. In contrast, when the equilibrium denaturation is observed by steady-state fluorescence emission intensity at 350 nm, two distinct transitions are observed. The first transition accounts for 60% of the observed signal and has a midpoint of 1.5 M GdnHCl. The second transition roughly parallels that observed by CD measurements with an approximate midpoint of 4.5 M GdnHCl. The near-UV CD spectrum, size-exclusion, and ultracentrifugation properties of [W_{B28},P_{B29}]insulin indicate that this analog does not self-associate in a concentration-dependent manner as does human insulin. Thus, the observed fluorescence changes must be due to specific conformational transitions which occur upon unfolding of the insulin monomer with the product of the first transition representing a stable folding intermediate of this molecule.

The characterization of the pathway(s) by which a protein folds to form a specific three-dimensional structure has been the subject of intense investigation throughout the past several decades. The highly cooperative nature of the equilibrium transition between the native (N) and denatured (D) forms of small globular proteins suggests that such transitions can be readily analyzed as a two-state phenomenon (N ↔ D). A detailed kinetic analysis of the pathway by which a protein proceeds from the denatured to native state has lead to the identification of discrete intermediates during the course of folding for several proteins (Kim & Baldwin, 1982). The existence of kinetic intermediates does not invalidate the two-state equilibrium model, in that these intermediates are transient and relatively unstable and are thus not appreciably populated under equilibrium conditions. However, several equilibrium intermediates have been identified which are sufficiently stable under partially denaturing conditions and are therefore amenable to structural analysis. One such intermediate has been described as a molten globule (Kuwajima et al., 1989; Ptitsyn, 1987). The molten-globule state is characterized by the presence of a significant degree of secondary structure folded into a compact hydrophobic core with a highly dynamic or fluctuating tertiary structure. A further understanding of the physical and chemical properties of folding intermediates is paramount to the development of a comprehensive theoretical model for protein folding.

The physicochemical properties of certain equilibrium folding intermediates can often lead to the irreversible aggregation of the protein through nonspecific intermolecular interactions. If the solution conditions chosen for the folding of a protein promote the accumulation of significant concentrations of such an intermediate, the formation of a nonproductive precipitate may constitute the major product of the folding reaction. An understanding of these types of side reactions to the folding process are particularly relevant when one considers the increasing number of proteins which are being examined as potential therapeutic agents for use in the treatment of a wide variety of disease states. The large-scale biosynthetic production of protein therapeutics often necessitates their extraction from a nonhomogeneous protein precipitate using high concentrations of chemical denaturants such as urea or guanidine hydrochloride (GdnHCl).[1] During the purification and processing of these proteins, the denaturant concentration must be adjusted to a level which facilitates the folding of the molecule. As previously mentioned, if an intermediate accumulates during the refolding process, the physical and conformational properties of the intermediate may dictate the final product of the reaction. The intermediate may involve the exposure of hydrophobic regions of the molecule which are normally buried, and valuable material may be lost as the result of hydrophobic-induced aggregation. The occurrence of an intermediate of this type has been well

* Author to whom correspondence should be addressed.
‡ Parenteral Products Research and Development.
⊥ Present address: Boehringer Mannheim Corp.
§ Physical Chemistry.
∥ Diabetes Research.

[1] Abbreviations: GdnHCl, guanidine hydrochloride; BHI, biosynthetic human insulin; HEPES, *N*-(2-hydroxyethylpiperazine)-*N*′-2-ethansulfonic acid; HPLC, high-performance liquid chromatography; CD, circular dichroism; EDTA, ethylenediaminetetraacetic acid; MRE, mean residue ellipticity; NMR, nuclear magnetic resonance.

0006-2960/92/0431-5692$03.00/0 © 1992 American Chemical Society

documented in the case of bovine growth hormone (Brems et al., 1986; Havel et al., 1986).

Insulin, a polypeptide hormone which is produced by the β-cells of the pancreatic islets of Langerhans, is intimately involved in the homeostasis of blood glucose levels. Changes in the primary structure of insulin have been identified which lead to the onset of diabetes mellitus (Tager et al., 1980; Haneda et al., 1984). As a result, insulin has been the subject of exhaustive investigation at the cellular and molecular levels. Indeed, insulin has served as a paradigm in the biophysical characterization of protein structure/function relationships. Biosynthetic human insulin (BHI) also represents the first recombinant protein to receive regulatory approval and to be subsequently marketed as a therapeutic agent. Although insulin is considered one of the best characterized proteins in terms of its structural properties, until recently very little has been reported concerning the folding or conformational stability of insulin. Past studies relating to the oxidative refolding of insulin have been hampered by the aggregation phenomena associated with high insulin concentrations or the nonspecific binding to surfaces which occurs at concentrations low enough to yield the monomeric form as the predominant species (Markussen & Heding, 1974; Steiner & Clark, 1968). We have recently initiated studies involving the characterization of the folding, intrinsic conformational dynamics, and stability of BHI (Brems et al., 1990). In an attempt to probe the local conformation and dynamics of BHI at specific sites within the tertiary structure, we have constructed an insulin analog in which a tryptophan residue has been strategically situated into the C-terminal domain of the insulin B-chain. The presence of this lone tryptophan residue offers a unique spectroscopic probe which is sensitive to local changes in the solution structure of the molecule. In addition, this analog incorporates an amino acid change in which proline B28 has been displaced and substituted at the B29 position ([W_{B28},P_{B29}]insulin). Amino acid changes of the latter type have been shown to yield insulin analogs which are monomeric under conditions which usually result in insulin aggregation (Frank et al., 1991).

Experimental Procedures

Materials. Ultrapure GdnHCl was purchased from ICN Biochemicals. HEPES buffer was of enzyme grade and was obtained from Fischer Scientific. Anhydrous absolute ethyl alcohol (200 proof) was supplied from Quantum Chemicals. *tert*-BOC-amino acids were purchased from Applied Biosystems Inc. Zinc-free BHI was obtained from Eli Lilly & Co. *N*-Acetyltryptophanamide was purchased from Sigma Chemical Co. All other chemicals were of analytical grade or higher.

Synthesis and Isolation of [W_{B28},P_{B29}]Insulin. An octapeptide of the sequence NH_2-Gly-Phe-Phe-Tyr-Thr-Trp-Pro-Thr-CO_2H was synthesized using an Applied Biosystems model 430A peptide synthesizer. The resulting octapeptide was purified by reverse-phase HPLC and the composition characterized by mass spectrometry and N-terminal sequence analysis. [W_{B28},P_{B29}]Insulin was prepared by coupling desoctapeptide (B23–30) porcine insulin, which is identical in sequence to desoctapeptide human insulin, with the above octapeptide using trypsin-assisted semisynthesis in a mixed organic solvent system (Kubiak & Cowburn, 1986). The analog was purified by gel filtration and reverse-phase HPLC and characterized by quantitative amino acid analysis, fast atom bombardment mass spectrometry, analytical reverse-phase HPLC, and size exclusion chromatography.

Biological Activity. The in vivo biological properties of insulin and the [W_{B28},P_{B29}]insulin analog were determined by quantifying the percent change in blood glucose in fasted normal male Sprague Dawley rats subsequent to subcutaneous administration of the test compound. Dose–response curves were constructed from experiments at five different concentrations of the compound using the maximal response (usually occurring 1 or 2 h postinjection). Five test animals and five control animals were used at each concentration. The subcutaneous dose (μg/kg) which yielded the half-maximal hypoglycemic response (ED_{50}) was determined from each dose–response curve and was taken as a measure of the in vivo potency of the particular test compound.

Circular Dichroism Spectroscopy. Circular dichroism measurements were taken on an AVIV 62D spectrometer. Near- and far-UV spectra were recorded in 20 mM HEPES and 1 mM EDTA, pH 7.5. Near-UV spectra were collected at 23 °C using a protein concentration of 1.00 mg/mL. Far-UV spectra were recorded using a 0.020-cm cell and a protein concentration of 0.1 mg/mL. In order to investigate the effect of protein concentration on the near-UV region of the CD spectra, the intensities at 275 nm were recorded as a function of protein concentration using samples of varying dilutions and cylindrical cells with path lengths ranging from 0.1 to 5.0 cm. Results are reported as mean residue ellipticity (MRE) having units of deg·cm^2·dmol^{-1} and were calculated using a mean residue mass of 115 Da.

Fluorescence Spectroscopy. Steady-state fluorescence measurements were obtained using an SLM-Aminco model 48000S spectrofluorometer. Fluorescence emission spectra were collected at 25 °C using a 1 cm × 1 cm cell. All samples were dissolved in 20 mM HEPES, 1 mM EDTA, and 20% ethanol (v/v), pH 7.5, and were filtered through a 0.2-μm filter prior to data acquisition. An excitation wavelength of 295 nm was used to specifically excite the single tryptophan present in the [W_{B28},P_{B29}]insulin analog. The fluorescence emission wavelength was scanned from 300 to 450 nm. The excitation and emission slits were set for a 4-nm band-pass. Spectra obtained for the appropriate solvent blanks were subtracted from all samples.

Equilibrium Denaturation Measurements. GdnHCl-induced equilibrium denaturation experiments were performed as previously described (Brems et al., 1990). Briefly, samples of varying GdnHCl concentrations were prepared by combining different ratios of denaturant stock solutions and a standard buffer composed of 20 mM HEPES, 1 mM EDTA, and 20% (v/v) ethanol, pH 7.5. The addition of 20% ethanol reduces the tendency of insulin to form dimers and higher ordered aggregates and thereby reduces the number of species present under native conditions such that a two-state model can be applied to the analysis of equilibrium denaturation experiments (Brems et al., 1990). The addition of 20% ethanol was found to be unnecessary for the analysis of monomeric insulin analogs; however, it was included to allow for a direct comparison to results obtained for human insulin.

Samples prepared for equilibrium denaturation measurements as followed by far-UV CD contained 0.10 mg/mL protein and were recorded using a 0.500-cm cuvette at 23 °C. The signal at 224 nm, indicative of the α-helical secondary structural content, was recorded as a function of GdnHCl concentration. Equilibrium denaturation measurements in which the intrinsic steady-state fluorescence intensity was observed were made at a protein concentration of 10 μM in a cuvette with a 1-cm path length at 23 °C.

Protein concentration determinations for [W_{B28},P_{B29}]insulin were calculated on the basis of the UV absorbance spectrum recorded on an AVIV model 14DS double-beam spectrophotometer. An extinction coefficient of 1.735 (mg/mL)$^{-1}$·cm^{-1}

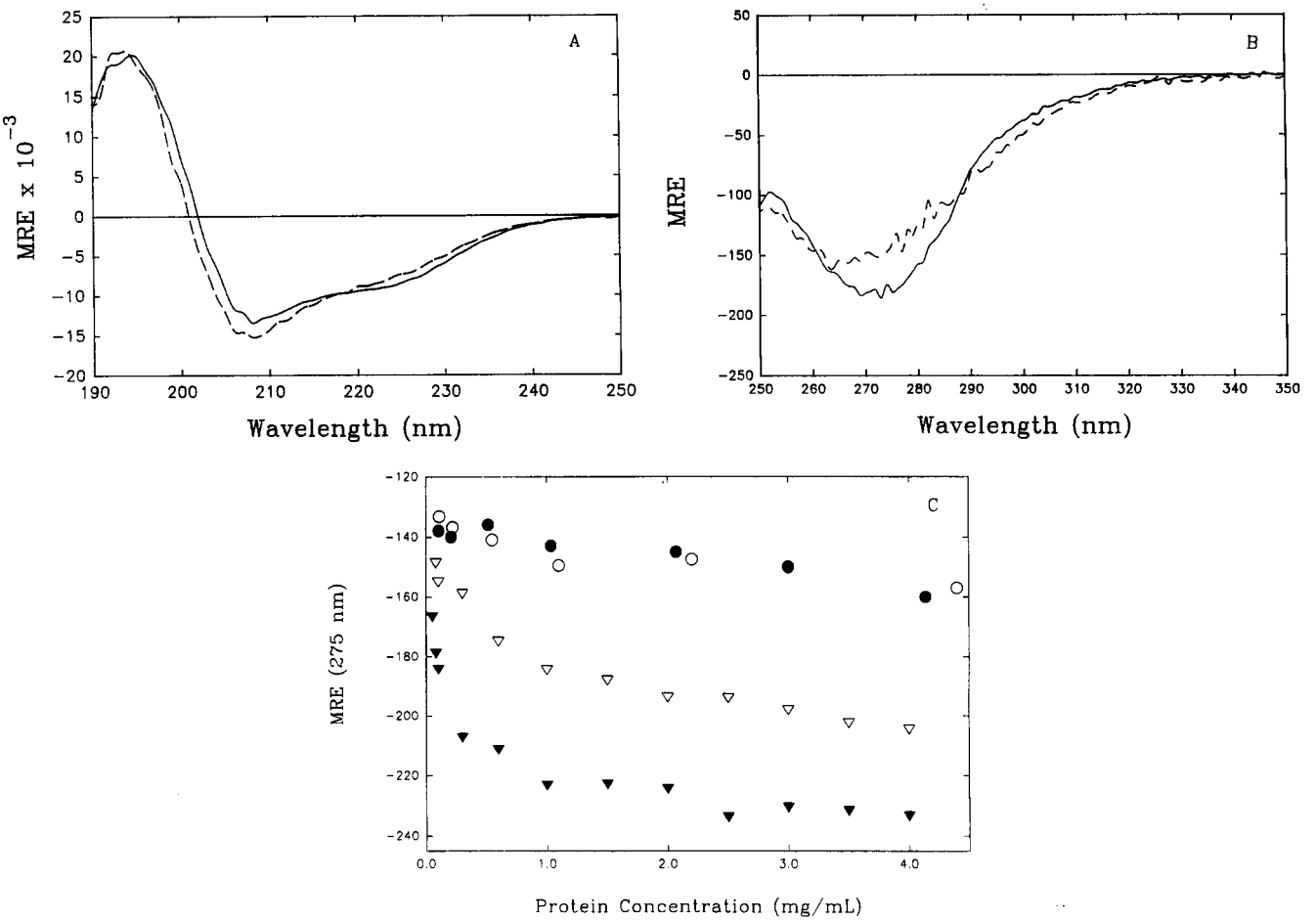

FIGURE 1: (A) Far- and (B) near-UV CD spectra for BHI (solid curve) and [W_{B28},P_{B29}]insulin (dashed curve) were collected as described under Experimental Procedures. The observed differences between the two molecules in both spectral regions are analogous to those seen in a comparison of certain monomeric insulin analogs with human insulin under similar solution conditions (Brems et al., 1991). (C) Effect of protein concentration on the CD signal at 275 nm of [W_{B28},P_{B29}]insulin, in the presence (open circles) and absence (closed circles) of 20% ethanol, and of BHI in the presence (open triangles) and absence (closed triangles) of 20% ethanol.

at 278 nm was calculated from the absorbance value recorded for a sample of known protein concentration, as previously determined by quantitative amino acid analysis. Concentrations of human insulin were determined by UV absorbance spectroscopy using an extinction coefficient of 1.05 (mg/mL)$^{-1}$·cm^{-1} at 276 nm (Frank et al., 1968).

Aggregation State Analysis. The aggregation state of the [W_{B28},P_{B29}]insulin analog was determined by HPLC size-exclusion chromatography and equilibrium ultracentrifugation. HPLC size-exclusion experiments were performed using a YMC pack PVA-SIL-120A column. The mobile phase was composed of 20 mM sodium phosphate, 0.2 M sodium chloride, and 0.001% NaN_3, pH 7.5. Samples of 100 μL were injected and eluted from the column at a flow rate of 1 mL/min. Distribution coefficients (K_d) were calculated for samples and a set of standard proteins based upon the elution volume of the protein as detected by UV absorbance at 278 nm as follows:

$$K_d = (V_e - V_o)/(V_t - V_o)$$

where V_e is the elution volume of the sample, V_o is the excluded volume of the column as determined by the elution of Blue Dextran, and V_t is the total volume of the column as determined by the elution of DL-dithiothreitol. The observed K_d was then used to calculate an apparent molecular weight of the sample.

Analytical equilibrium ultracentrifugation was accomplished using a Spinco model E analytical ultracentrifuge with a photoelectric scanning optical system operating at 22 °C. Samples were dissolved in either 50 mM NaCl and 50 mM Na_2HPO_4, pH 7.2, or 100 mM HEPES, 1 mM EDTA, and 20% ethanol, pH 7.5. The weight average molecular weight was calculated assuming ideal solution conditions (Frank & Veros, 1968).

RESULTS

Analog Synthesis. The [W_{B28},P_{B29}]insulin analog used in the present study was synthesized by an enzymatic semisynthetic method (Kubiak & Cowburn, 1986). The major product of the reaction was purified to apparent homogeneity as indicated by the presence of a single peak upon reverse-phase HPLC chromatographic analysis. Mass spectral data indicated that the synthesized molecule had a mass of 5866.2, which is in excellent agreement with a theoretical value of 5866.7. Hydrolysis of the compound in the presence of trace amounts of thioglycolic acid followed by quantitative amino acid analysis indicated the presence of a single tryptophan residue with no other changes in the theoretical amino acid composition.

Biological Activity. The rat hypoglycemic effect elicited by human insulin and [W_{B28},P_{B29}]insulin were essentially equivalent based upon ED_{50} values of 7.8 μg/kg and 7.5 μg/kg for BHI and [W_{B28},P_{B29}]insulin, respectively.

Spectroscopic Characterization. The far-UV CD spectra of zinc-free human insulin and [W_{B28},P_{B29}]insulin are shown in Figure 1A. Although the spectra for insulin and [W_{B28},P_{B29}]insulin are similar, discrete differences were noted. The observed differences involve a minor decrease in the

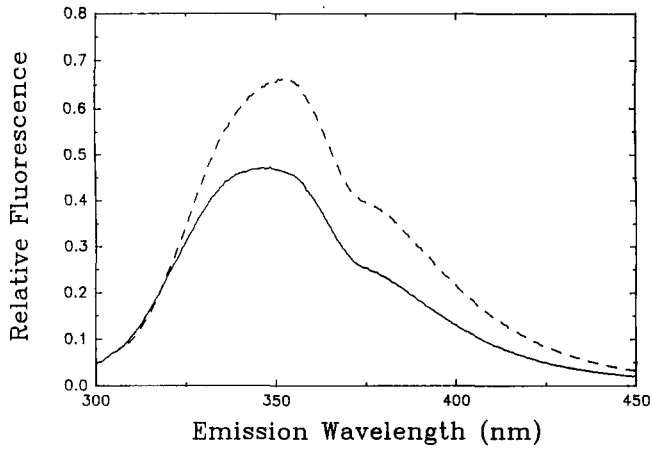

FIGURE 2: Steady-state fluorescence emission spectrum of [W_{B28},P_{B29}]insulin in the native (solid curve) and denatured states (dashed curve) were recorded using an excitation wavelength of 295 nm and band-passes of 4 nm for both the excitation and emission beams. The spectra were corrected for background with a solvent blank and normalized to the intensity observed with an equimolar concentration of the model compound *N*-acetyltryptophanamide under identical solution conditions.

negative ellipticity at approximately 225 nm and a small increase in the negative ellipticity at 208 nm. These spectral shifts are similar to those observed between human insulin and other insulin analogs in which the natural sequence of -(Pro–Lys)- has been changed to -(Xaa–Pro)- at the B28 and B29 positions, respectively (Frank et al., 1991). The near-UV CD spectra of [W_{B28},P_{B29}]insulin also differs from that of human insulin as shown in Figure 1B. The changes in this region of the CD spectra involve a decrease in the negative ellipticity and a shift in the minimum wavelength from 275 to 268 nm. Figure 1C reveals that the CD signal at 275 nm for [W_{B28},P_{B29}]insulin is independent of the protein concentration in both the presence and absence of 20% ethanol. In contrast, the CD signal at 275 nm for BHI was found to vary as a function of protein concentration in the absence of ethanol. The addition of 20% ethanol to the buffer system diminishes the overall magnitude of the concentration dependent signal change but does not completely eliminate the phenomenon.

The steady-state fluorescence spectra of [W_{B28},P_{B29}]insulin, in the presence and absence of denaturing levels of GdnHCl, are presented in Figure 2. The data were normalized as a percentage of the fluorescence intensity observed for an equimolar concentration (molar tryptophan content) of the model compound *N*-acetyltryptophanamide under identical solution conditions. A 20% increase in the relative fluorescence intensity is seen upon the addition of GdnHCl at concentrations which have previously been found to fully denature human insulin (Brems et al., 1990). However, the maximum fluorescence intensity observed is only 70% of that expected by comparison to the model compound *N*-acetyltryptophanamide. A slight red-shift in the wavelength maximum, from 347 to 350 nm, accompanies the increase in fluorescence intensity upon denaturation of the protein.

Equilibrium Denaturation. Results of the GdnHCl-induced equilibrium denaturation of [W_{B28},P_{B29}]insulin are presented in Figure 3. The changes observed by circular dichroism intensity at 224 nm revealed a single cooperative transition with a Gibbs free energy of unfolding of 3.9 kcal/mol and a midpoint occurring at 4.9 M GdnHCl when analyzed by the linear extrapolation method of Pace (1975). The changes observed by steady-state fluorescence intensity at 350 nm were more complex in that an inflection is seen between 3 and 4

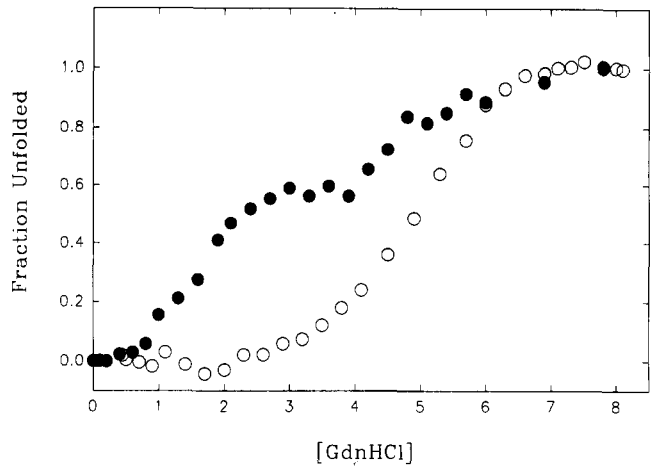

FIGURE 3: Equilibrium denaturation of [W_{B28},P_{B29}]insulin as followed by the far-UV CD intensity at 224 nm (open circles) and steady-state fluorescence emission intensity at 350 nm (filled circles). The raw data have been normalized as the fraction of the signal observed for the unfolded protein.

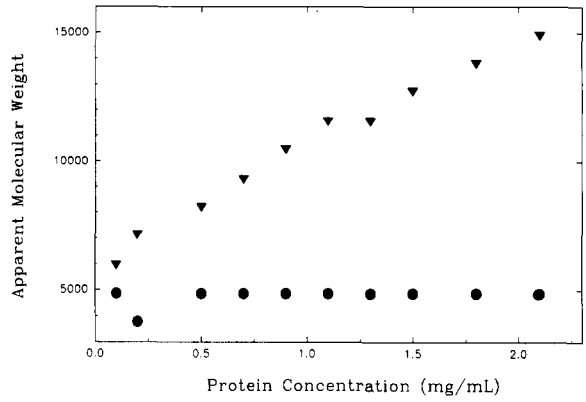

FIGURE 4: Effect of protein concentration on the apparent molecular weight of BHI (triangles) and [W_{B28},P_{B29}]insulin (circles) during size-exclusion chromatography. The apparent molecular weight was determined by a comparison of the elution volume of the sample relative to those observed for [K_{B28},P_{B29}]insulin (5.6 kDa), ribonuclease A (13.7 kDa), chymotrypsinogen A (25 kDa), and ovalbumin (43 kDa). The elution volume was expressed as a distribution coefficient, $K_d = (V_e - V_o)/(V_t - V_o)$, where V_e is the elution volume of the sample, V_o is the excluded volume, and V_t is the total column volume.

M GdnHCl indicating the presence of two distinct transitions. The initial transition, which accounts for approximately 60% of the total fluorescence intensity change, is sigmoidal in nature and is centered at 1.5 M GdnHCl. The second transition is broad and occurs with a midpoint at approximately 4.5 M GdnHCl. This second transition appears to coincide with the changes observed by far-UV CD and thus represents the global unfolding of the molecule.

Aggregation State Analysis. The tendency of insulin to self-associate as the result of specific intermolecular interactions necessitates the determination of the aggregation state of insulin and [W_{B28},P_{B29}]insulin for a proper structural interpretation of the spectroscopic results. Size-exclusion chromatographic analysis of BHI and [W_{B28},P_{B29}]insulin in the absence of ethanol are presented in Figure 4. A concentration-dependent increase in the apparent molecular weight of BHI is observed, indicating an increase in the hydrodynamic volume as the result of aggregation. The lack of concentration-dependence on the apparent molecular weight for [W_{B28},P_{B29}]insulin indicates a decreased tendency toward self-association for this analog, relative to human insulin.

An assessment of the degree of aggregation for BHI and [W_{B28},P_{B29}]insulin, both in the presence and absence of 20%

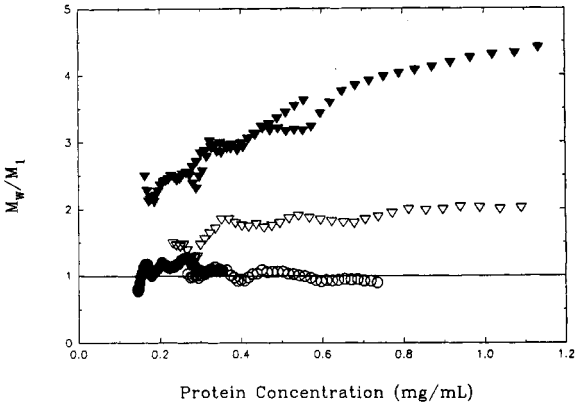

FIGURE 5: Analytical ultracentrifugation analysis of the aggregation state of BHI and [W_{B28},P_{B29}]insulin. The variation in the weight average molecular weight (M_W) relative to the monomer molecular weight (M_1) as a function of protein concentration was determined for BHI in the presence (open triangles) and absence (closed triangles) of 20% (v/v) ethanol, and for [W_{B28},P_{B29}]insulin in the presence (open circles) and absence (closed circles) of 20% (v/v) ethanol.

ethanol as determined by analytical equilibrium ultracentrifugation, are presented in Figure 5. A concentration-dependent increase in the aggregation state is clearly observed for BHI in the absence of ethanol. This phenomenon is diminished in the presence of 20% ethanol; however, the predominant species appears to be dimeric above protein concentrations of 0.5 mg/mL. In contrast, analysis of [W_{B28},P_{B29}]insulin yielded a weight average molecular weight of 1.13 relative to the monomer molecular weight both in the presence and absence of 20% ethanol. Thus, no appreciable aggregation was observed for [W_{B28},P_{B29}]insulin.

DISCUSSION

The purpose of the present study was to characterize the local conformational properties of the C-terminal region of the insulin B-chain. The strategy employed involved the synthesis of an insulin analog in which a tryptophan residue was placed within this portion of the molecule. The fluorescence properties of tryptophan residues are quite sensitive to the local environment of the aromatic side chain. Thus, in the absence of other chromophores with similar spectroscopic properties, i.e., multiple tryptophan residues or aromatic cofactors, the characteristic fluorescence spectra of a protein can yield specific information concerning the conformational properties within the immediate region of the fluorophore. A similar approach using recombinant DNA technology has been utilized recently in successfully addressing the conformational properties of specific regions within several proteins (Atkins et al., 1991; Gardner & Matthews, 1990; Eftink et al., 1991; Smith et al., 1991).

Analytical characterization of the [W_{B28},P_{B29}]insulin analog by mass spectroscopy, amino acid analysis, and N-terminal sequence analysis of the octapeptide employed in the synthesis of the molecule indicate that the prepared analog was of the desired composition and sequence. The far-UV CD spectra presented in Figure 1A suggests that the [W_{B28},P_{B29}]insulin analog and human insulin have similar secondary structural content. Furthermore, [W_{B28},P_{B29}]insulin exhibits in vivo biological activity similar to that of native human insulin, indicating that [W_{B28},P_{B29}]insulin must attain a solution conformation similar to that of human insulin. As seen in Figure 1B, the near-UV CD spectrum of [W_{B28},P_{B29}]insulin differs from that of human insulin in both the intensity and the wavelength of the ellipticity minimum. A decrease in the negative intensity within this region of the spectrum has been interpreted as an indication of a decreased tendency toward self-association or aggregation for insulin (Rupley et al., 1967; Strickland & Mercola, 1976). This interpretation is further supported by experiments designed to ascertain the aggregation state of human insulin and [W_{B28},P_{B29}]insulin. Figure 1C shows that the CD signal at 275 nm for human insulin is modulated in a concentration-dependent manner. The addition of 20% ethanol has been previously found to eliminate any concentration-dependent changes in the equilibrium denaturation profiles for BHI as determined by near-UV CD spectroscopy (Brems et al., 1990). Indeed, the relative change in the CD signal at 275 nm due to varying protein concentration was significantly diminished in the presence of 20% ethanol. A similar trend in the aggregation state of BHI is observed using analytical ultracentrifugation and size-exclusion chromatography. Thus, it appears that changes in the CD signal at 275 nm correlate with the observed changes in the aggregation state of human insulin. The CD signal at 275 nm for [W_{B28},P_{B29}]insulin was independent of the protein concentration in either the presence or absence of 20% ethanol. Results from equilibrium ultracentrifugation also indicate that [W_{B28},P_{B29}]insulin is monomeric in both the presence and absence of added ethanol. Thus, it is concluded that any changes in the fluorescence properties of [W_{B28},P_{B29}]insulin cannot be attributed to changes in the aggregation state of the molecule.

The wavelength maximum of the steady-state fluorescence emission intensity for native [W_{B28},P_{B29}]insulin occurs at 347 nm. The wavelength of the maximum emission intensity for tryptophan is known to be sensitive to the hydrophobic nature of the local environment. A red-shift from approximately 335 to 350 nm has been correlated with the transition of the residue from a buried or hydrophobic environment to a solvent-exposed or hydrophilic environment (Lakowicz, 1973). Thus, the data suggest that the tryptophan residue in [W_{B28},P_{B29}]insulin is in an environment which is hydrophilic and is therefore presumed to be exposed to bulk solvent. High-resolution X-ray crystallographic studies of the 2-Zn BHI hexamer indicate that segment B24–26 assumes a β-sheet fold and constitutes an intermolecular interface between insulin monomers within an asymmetric dimer (Baker et al., 1988). The C-terminal region of the B-chain has also been identified as an important site of interaction between monomers under solution conditions which favor the formation of insulin dimers or higher ordered aggregate species (Strickland & Mercola, 1976). Recent studies which explored the self-association properties of various insulin analogs modified by either amino acid substitution or truncation have also implicated this region of the molecule as an important determinant in modulating intermolecular aggregation (Frank et al., 1991). These studies have aided in the design of monomeric insulins with clinically altered properties (Howey et al., 1991). Molecular dynamics calculations on the individual crystallographic protomers (Krüger et al., 1987) and 2D ^{1}H NMR studies of insulin under solution conditions which yield the monomer species (Weiss et al., 1989; Roy et al., 1990a) suggest that while critical contacts between the C-terminal region of the B-chain and the core of the molecule are present, this segment of the molecule exists in an extended conformation in solution, is highly flexible, and is exposed to solvent. Thus, the wavelength at which the fluorescence emission intensity maximum occurs for [W_{B28},P_{B29}]insulin is consistent with the proposed conformation of this region in the insulin monomer. The magnitude of the fluorescence intensity increased approximately 20% upon unfolding due to the addition of GdnHCl. However, the

fluorescence intensity of denatured [W_{B28},P_{B29}]insulin is still only 70% of that seen for an equimolar solution of the model compound *N*-acetyltryptophanamide. A possible explanation for the residual quenching phenomena in the denatured state may reside in the sequence-dependent proximity of the tryptophan residue to the aromatic triplet, phenylalanine B24 and B25, and tyrosine B26.

Results from the GdnHCl-induced equilibrium denaturation of [W_{B28},P_{B29}]insulin as determined by the far-UV CD intensity at 224 nm indicate a slight decrease in the stability of this analog, as judged by the midpoint of the transition and the calculated Gibbs free energy of unfolding, relative to human insulin (Brems et al., 1990). Recent experiments, in which the thermodynamic stability was determined for several of the [X_{B28},P_{B29}]insulin analogs, failed to reveal any specific correlation between the physical properties of the residue at position B28 and the inherent stability of each analog (Brems et al., 1991). Thus, it is difficult to speculate as to the reason for the minor decrease in the stability of [W_{B28},P_{B29}]insulin. The equilibrium denaturation of [W_{B28},P_{B29}]insulin, as observed by changes in the steady-state fluorescence intensity, demonstrates a clear inflection in the denaturation transition. The sigmoidal transition observed between 1 and 3 M GdnHCl (Figure 3) occurs at GdnHCl concentrations that are nondenaturing as determined by the far-UV CD signal at 224 nm. The presence of a distinct inflection in the transition from the native to denatured states, and the noncoincidence of transitions observed by different techniques, constitutes direct evidence for the existence of a discrete folding intermediate which is populated under equilibrium conditions (Kim & Baldwin, 1982). Thus, the C-terminal region of the B-chain undergoes a distinct conformational change prior to the loss of the major secondary structural elements. This conformational transition results in a populated equilibrium folding intermediate. Preliminary NMR studies of the temperature-dependent changes in the chemical shifts of residues widely dispersed throughout the molecule suggest that multiple folding intermediates may exist (Weiss et al., 1989). It appears that the forces which stabilize the local conformation within the C-terminal portion of the B-chain are relatively weak. It is suggested that this region of the molecule may be quite flexible and exist in multiple conformational substates. This interpretation of the data is consistent with several other lines of evidence. Detailed crystallographic studies have shown that the predominant feature of insulin's three-dimensional structure involves the packing of the three helical segments. However, differences between molecules present within a single crystal form, and between molecules in different crystal forms, indicate that multiple conformations are accessible (Chothia et al., 1983). These observed differences primarily involve movements of multiple side chains and the main-chain conformation within the N- and C-termini of the insulin B-chain. In addition, molecular dynamics simulations indicate that the hydrophobic core of the molecule is essentially static, while distinct conformational fluctuations occur within the N- and C-termini (Krüger et al., 1987). The observed conformational heterogeneity within the C-terminal region of the B-chain has been taken as an indication that flexibility may exist within this portion of the molecule. Recent NMR investigations on the solution structure of insulin (Weiss et al., 1989; Roy et al., 1990b; Kline & Justice, 1990), proinsulin (Weiss et al., 1990), and des-pentapeptide insulin (Hua & Weiss, 1990; Bolens et al., 1990; Hua et al., 1989, 1991) have shown the presence of conformational substates involving flexibility within the C-terminal region of the B-chain. Numerous studies involving insulin analogs with the C-terminus of the B-chain truncated, chemically cross-linked to the N-terminus of the A-chain, or altered by amino acid substitution have also implicated a role for conformational flexibility in the interaction of insulin with its cell surface receptor (Nakagawa & Tager, 1987, 1989; Casaretto et al., 1987; Mirmira & Tager, 1989). One proposal recently set forth suggests that the receptor-bound conformation of insulin involves the partial unfolding of the B-chain C-terminal region in order to expose critical sites of interaction between insulin and the receptor (Derewenda et al., 1991).

In conclusion, we present evidence for the existence of a populated folding intermediate for the monomeric analog [W_{B28},P_{B29}]insulin. The results of the present study are consistent with the current hypothesis in which the C-terminal region of the insulin B-chain is quite flexible and highly dynamic with regard to its inherent motion. Further studies of this type will be required to address the local conformational properties of other regions within the insulin molecule. Finally, a characterization of the biophysical properties of the identified intermediate will be required to determine if it is similar to other stable folding intermediates which are of a molten globule nature.

Acknowledgments

We are grateful to Dr. Walter Shaw for determining the in vivo biological potency of [W_{B28},P_{B29}]insulin.

References

Atkins, W. M., Stayton, P. S., & Villafranca, J. J. (1991) *Biochemistry 30*, 3406–3416.

Baker, E. N., Blundell, T. E., Cutfield, G. S., Cutfield, S. M., Dodson, E. J., Dodson, G. G., Hodgkin, D. M. C., Hubbard, R. E., Iassac, W. M., Reynolds, D. C., Sakabe, K. S., Sakabe, N., & Vjayan, N. M. (1988) *Philos. Trans. R. Soc. London B319*, 369–456.

Brems, D. N., Plaisted, S. M., Kauffman, E. W., & Havel, H. A. (1986) *Biochemistry 25*, 6539–6543.

Brems, D. N., Brown, P. L., Heckenlaible, L. A., & Frank, B. H. (1990) *Biochemistry 29*, 9289–9293.

Brems, D. N., Bryant, C., Chance, R. E., Shields, J. E., & Frank, B. H. (1991) *Diabetes 40 (Suppl. 1)*, 423A.

Bolens, R., Ganadu, M. L., Verheyden, P., & Kaptein, R. (1990) *Eur. J. Biochem. 191*, 147–153.

Casaretto, M., Spoden, M., Diaconesu, C., Gattner, H. G., Zahn, H., Brandenburg, D., & Wollmer, A. (1987) *Biol. Chem. Hoppe-Seyler 368*, 709–716.

Chothia, C., Lesk, A. M., Dodson, G. G., & Hodgkin, D. C. (1983) *Nature 302*, 500–505.

Derewenda, U., Derewenda, Z., Dodson, E. J., Dodson, G. G., Bing, X., & Markussen, J. (1991) *J. Mol. Biol. 220*, 425–433.

Eftink, M. R., Ghiron, C. A., Kautz, R. A., & Fox, R. O. (1991) *Biochemistry 30*, 1193–1199.

Frank, B. H., & Veros, A. J. (1968) *Biochem. Biophys. Res. Commun. 32*, 155.

Frank, B. H., Veros, A. J., & Pekar, A. H. (1972) *Biochemistry 11*, 4926–4931.

Frank, B. H., Brems, D. N., Chance, R. E., DiMarchi, R. D., & Shields, J. E. (1991) *Diabetes 40 (Suppl. 1)*, 423A.

Gardner, J. A., & Matthews, K. S. (1990) *J. Biol. Chem. 265*, 21061–21067.

Haneda, M., Polonsky, K. S., Bergenstal, R. M., Jaspan, J. B., Shoelson, S. E., Blix, P. M., Chan, S. J., Kwok, S. C. M., Wishner, W. B., Zeidler, A., Olefsky, J. M., Friedemberg, G., Tager, H., Steiner, D. F., & Rubenstein, A. H.

(1984) *N. Engl. J. Med. 310*, 1288-1294.
Havel, H. A., Kauffman, E. W., Plaisted, S. M., & Brems, D. N. (1986) *Biochemistry 25*, 6533-6538.
Howey, D. C., Hooper, S. A., & Bowsher, R. R. (1991) *Diabetes 40 (Suppl. 1)*, 423A.
Hua, Q. X., & Weiss, M. A. (1990) *Biochemistry 29*, 10545-10555.
Hua, Q. X., Chen, Y. J., Wang, C. C., Wang, D. C., & Roberts, G. C. K. (1989) *Biochim. Biophys. Acta 994*, 114-120.
Hua, Q. X., Shoelson, S. E., Kochoyan, M., & Weiss, M. A. (1991) *Nature 354*, 238-241.
Kim, P. S., & Baldwin, R. L. (1982) *Annu. Rev. Biochem. 51*, 459-489.
Kline, A. D., & Justice, R. M. (1990) *Biochemistry 29*, 2906-2913.
Krüger, P., Strassbburger, W., Wollmer, A., vanGunsteren, W. F., & Dodson, G. G. (1987) *Eur. Biophys. J. 14*, 449-459.
Kubiak, T., & Cowburn, D. (1986) *Int. J. Pept. Protein Res. 27*, 514-521.
Kuwajima, K. (1989) *Proteins: Struct., Funct., Genet. 6*, 87-103.
Lakowicz, J. R. (1983) *Principles of Fluorescence Spectroscopy*, Plenum Press, New York.
Markussen, J., & Heding, L. G. (1974) *Int. J. Pept. Protein Res. 6*, 245-252.
Mirmira, R. G., & Tager, H. S. (1989) *J. Biol. Chem. 264*, 6349-6354.
Nakagawa, S. H., & Tager, H. S. (1987) *J. Biol. Chem. 262*, 12054-12058.
Nakagawa, S. H., & Tager, H. S. (1989) *J. Biol. Chem. 264*, 272-279.
Pace, C. N. (1975) *CRC Crit. Rev. Biochem. 3*, 1-100.
Ptitsyn, O. B. (1987) *J. Protein Chem. 6*, 273-293.
Roy, M., Lee, R. W. K., Brange, J., & Dunn, M. F. (1990a) *J. Biol. Chem. 265*, 5448-5452.
Roy, M., Lee, R. W. K., Kaarsholm, N. C., Thogersen, H., Brange, J., & Dunn, M. F. (1990b) *Biochim. Biophys. Acta 1053*, 63-73.
Rupley, J. A., Renthal, R. D., & Praissman, M. (1967) *Biochim. Biophys. Acta 140*, 185-187.
Smith, C. J., Clarke, A. R., Chia, W. N., Ifront, L. I., Atkinson, T., & Holbrook, J. J. (1991) *Biochemistry 30*, 1028-1036.
Steiner, D. F., & Clark, J. L. (1968) *Proc. Natl. Acad. Sci. U.S.A. 60*, 622-629.
Strickland, E. H., & Mercola, D. (1976) *Biochemistry 15*, 3875-3884.
Tager, H., Thomas, N., Assoian, R., Rubenstein, A., Saekow, M., Olefsky, J., & Kaiser, E. T. (1980) *Proc. Natl. Acad. Sci. U.S.A. 77*, 3181-3185.
Weiss, M. A., Nguyen, D. T., Khait, I., Inouye, K., Frank, B. H., Beckage, M., O'Shea, E., Shoelson, S. E., Karplus, M., & Neuringer, L. J. (1989) *Biochemistry 28*, 9855-9873.
Weiss, M. A., Frank, B. H., Khait, I., Pekar, A., Heiney, R., Shoelson, S. E., & Neuringer, L. J. (1990) *Biochemistry 29*, 8389-8401.

Similarities in Melittin Functional Group Reactivities during Self-Association and Association with Lipid Bilayers†

R. P. Oomen*,‡ and H. Kaplan§

Connaught Centre for Biotechnology Research, 1755 Steeles Avenue West, Willowdale, Ontario, Canada M2R 3T4, and Department of Chemistry, Faculty of Science, University of Ottawa, Ottawa, Ontario, Canada K1N 6N5

Received June 19, 1991; Revised Manuscript Received April 10, 1992

ABSTRACT: Competitive labeling of melittin over a range of concentrations in the presence and absence of liposomes provides a series of "snapshots" of the chemical reactivities of melittin's intrinsic nucleophiles. Distinct trends in apparent reactivities were observed for the Gly-1 α-amino group and the ϵ-amino groups of Lys-7 and Lys-21 and -23, over a range of concentrations, providing evidence for different forms of associated melittin in solution. The monomer–tetramer transition can be followed, in accord with structural details derived from X-ray crystallography. The reactivity behavior of the α-amino group of Gly-1 and the ϵ-amino groups of Lys-21 and Lys-23 suggests these groups undergo similar perturbations in their microenvironments during the monomer–tetramer transition in free solution. Similar changes in reactivity behavior occur upon association of melittin monomers with bilayer-forming lipids. Together, these findings suggest that the local environments of the N- and C-terminal segments have similar physicochemical properties in both the solution tetramer and the lipid-associated complex. The concentration dependence of the chemical properties of melittin is correlated with surface accessibility calculations which are used to provide a framework for interpretation. Aspects of several previously proposed models of membrane lysis can be accounted for by concentration-dependent properties of melittin.

The 26 amino acid peptide melittin is a potent α-helical cytotoxin comprising up to 50% of the dry weight of honeybee venom (King et al., 1976) and is frequently used to study protein–lipid interactions. Numerous mechanisms have been proposed to explain melittin's association with biological membranes and their consequent physical disruption, but the dynamic processes underlying these events remain poorly understood. Earlier models of melittin association with bilayers include surface adsorption (Schoch & Sargent, 1980), partial or full insertion (Terwilliger et al., 1982; Vogel et al., 1983), channel or pore formation (Tosteson & Tosteson, 1981; Vogel

† This work was supported by the National Science and Engineering Research Council of Canada.

‡ Present address: Connaught Centre for Biotechnology Research, 1755 Steeles Ave. W., Willowdale, Ontario, Canada M2R 3T4.
§ University of Ottawa.

0006-2960/92/0431-5698$03.00/0 © 1992 American Chemical Society